

The Use of Bred Vectors in the NCEP Global 3D Variational Analysis System

ZHAO-XIA PU,* EUGENIA KALNAY, DAVID PARRISH, WANSHU WU,⁺ AND ZOLTAN TOTH⁺

Environmental Modeling Center, National Centers for Environmental Prediction, NWS/NOAA, Washington, D.C.

1 October 1996 and 28 April 1997

ABSTRACT

The errors in the first-guess (forecast field) of an analysis system vary from day to day, but, as in all current operational data assimilation systems, forecast error covariances are assumed to be constant in time in the NCEP operational three-dimensional variational analysis system (known as a spectral statistical interpolation or SSI). This study focuses on the impact of modifying the error statistics by including effects of the “errors of the day” on the analysis system. An estimate of forecast uncertainty, as defined from the bred growing vectors of the NCEP operational global ensemble forecast, is applied in the NCEP operational SSI analysis system. The growing vectors are used to estimate the spatially and temporally varying degree of uncertainty in the first-guess forecasts used in the analysis. The measure of uncertainty is defined by a ratio of the local amplitude of the growing vectors, relative to a background amplitude measure over a large area. This ratio is used in the SSI system for adjusting the observational error term (giving more weight to observations in regions of larger forecast errors). Preliminary experiments with the low-resolution global system show positive impact of this virtually cost-free method on the quality of the analysis and medium-range weather forecasts, encouraging further tests for operational use. The results of a 45-day parallel run, and a discussion of other methods to take advantage of the knowledge of the day-to-day variation in forecast uncertainties provided by the NCEP ensemble forecast system, are also presented in the paper.

1. Introduction

A three-dimensional variational data assimilation system (3D VAR), known as the spectral statistical interpolation (SSI) analysis system was implemented operationally into the global forecasting system in 1991 at the National Centers for Environmental Prediction (NCEP, formerly the National Meteorological Center) (Parrish and Derber 1992; Derber et al. 1991). This advanced data assimilation scheme has played a vital role in recent data assimilation and research at NCEP and is still under development (Derber and Wu 1996; Parrish et al. 1997; Derber et al. 1994). The analysis is performed every 6 h and the 6-h forecast field is used as a first guess or background in the system. As in all general variational data assimilation systems, the objective function to minimize is defined as (Lorenz 1986)

$$2J = (x - x_b)^T \mathbf{B}^{-1} (x - x_b) + [K(x) - y]^T \mathbf{O}^{-1} \times [K(x) - y] + J_c, \quad (1)$$

where x is the analysis variable, x_b is the first guess, and y is the observational vector. Here, \mathbf{B} and \mathbf{O} denote the 6-h forecast and observational error covariance matrices, respectively; K is a “forward” operator that transforms analysis variables (such as temperature or vorticity) into simulated observations (such as velocities or radiances); and J_c denotes a dynamical constraint penalty that enforces a global balance of the analysis increments. This system is used to find an analysis field that best fits both the first guess and observations. It assumes that the forecast error and observation error are not correlated. The error covariance matrices \mathbf{B} and \mathbf{O} are currently held constant in time. However, the uncertainties in the first guess do change from day to day. It is therefore necessary to modify such covariance weights (Wahba et al. 1995). It is our purpose to investigate the impact of modifying the error statistics by introducing the effect of “errors of the day,” a problem identified as high priority in data assimilation (Kalnay and Toth 1994; Pu et al. 1997).

Iyengar et al. (1996) presented evidence indicating that the bred vectors used in the NCEP operational global ensemble forecast system (Toth and Kalnay 1993, 1995) represent reasonably well the magnitude and the horizontal and vertical distribution of analysis uncertainty in a statistical sense, averaged over longer time periods. They also found that the bred ensemble can capture well the flow-dependent errors of the day: the magnitude of the first-guess error correlates well with the spread in the ensemble. Zhu et al. (1996) generate

* Current affiliation: UCAR Visiting Scientist, NCEP, Washington, D.C.

⁺ Current affiliation: General Sciences Corporation, Laurel, Maryland.

Corresponding author address: Zhao-Xia Pu, EMC/NCEP2, WWB, Room 207, 5200 Auth Road, Camp Springs, MD 20746.
E-mail: wdzozp@sun1.wwb.noaa.gov

and verify probabilistic forecasts from the ensemble, and the scores are quite good at short lead time. Based on their results, the large spread in the short-range ensemble forecasts usually can be used to point out areas of large uncertainty in the first guess. Kalnay and Toth (1994) modified the first guess in such a way that the distance between the the first guess and the observations was minimized along the direction of the local bred vectors. This elimination of the bred vectors' projection on the first-guess error resulted in improved analyses, with a significant positive impact upon the forecasts, indicating that the ensemble provides information about growing errors in the first guess.

In this study, we will introduce the use of bred growing vectors of the NCEP operational global ensemble forecast (Toth and Kalnay 1993, 1995) into the NCEP SSI analysis system. It will be used to estimate the degree of uncertainty in the first guess that is related to dynamically conditioned, fast-growing errors. We will assume that this part of the first-guess error field can be well estimated by the ensemble spread.¹ Since currently the background error covariance in the SSI is cast in spectral and not in physical space, the spatial impact of large forecast error is done in a simpler fashion by modifying the observational error covariance, which is defined in physical space.

2. Methodology

To adjust geographically the covariances (which determine the weight of the observations in the variational data assimilation) by the error of the day, we define a scalar factor based on the NCEP ensemble forecasts measuring the uncertainties in first guess (forecast field).

The initial perturbation amplitudes in the NCEP ensemble forecast are forced to be spatially varying on a very large horizontal scale: they are smaller in data-rich continents, and larger over oceans, in order to make them proportional to the average analysis error. In addition to these fixed, continental-scale variations in amplitude, there are smaller areas of large spread of the ensemble forecasts, usually occupying a more local region, which vary from day to day. When we refer to a large uncertainty in a local area, we imply that the spread is larger in the local area than in the continental-scale background area (reference area). In this study, we estimate the spatially and temporally varying degree of uncertainty in the first-guess forecast by 24-h operational global ensemble forecasts. In order to eliminate the continental-scale, forced-amplitude differences, we define the spread as a ratio of the local amplitude of the growing vectors, relative to a reference amplitude measured over a large area:

$$\sigma^2 = \frac{\sum_{i=1}^n T_S(F_i - F_c)^2}{\sum_{i=1}^n T_L(F_i - F_c)^2} = \frac{\text{Spread (small scale)}}{\text{Spread (continental scale)}}, \quad (2)$$

where σ^2 is the ratio and it is defined in grid space; T denotes a smoothing convolution that is performed using spectral transforms (Purser et al. 1994); F represents the 24-h forecast at the same verification time; subscripts i and c denote the ensemble member and control forecast (operational forecast) respectively²; and n is the total number of ensemble members. Here, L and S denote the large scale (reference) and small scale (local) used in the smoothing operator. As indicated above, the ratio between the small-scale and the continental-scale ensemble spreads is introduced in (2) in order to capture only the day-to-day variation in forecast uncertainty, rather than the time-averaged distribution of analysis errors. When the ratio is large, there is more uncertainty in the first guess, and we assume that the guess field (6-h forecast) is likely to have larger error in these areas. Since it is difficult to introduce geographically localized adjustments into the background error \mathbf{B} because it is defined spectrally, instead, we give more weight to observational data in areas of large uncertainty by directly dividing the observation error variance by σ^2 , whenever this factor is greater than 1. Hence the analysis is driven closer to the data in these areas than in other areas. If the ratio is smaller than 1 (the forecast uncertainty is small), the observation error is maintained without change at its nominal value.

3. A numerical experiment

The method is tested in the current operational SSI analysis and medium-range forecast system. The model used in experiments is the same as the NCEP operational global spectral model, but with lower horizontal resolution, T62 with 28 sigma vertical levels (Pan et al. 1995). In the data assimilation cycle, an analysis is performed every 6 h. The NCEP ensemble forecast system is also performed in a T62 L28 version, and it generates five pairs of ensemble forecast members (Toth and Kalnay 1995) at 0000 UTC and two pairs of ensemble members at 1200 UTC.

As described in (2), the value of σ^2 is the ratio of mean square averages over the members of ensemble pairs and it will depend on the number of the ensemble members that are used in the computational procedure. In our experiment, because there are only two pairs ensemble forecast available for 1200 UTC and there is no ensemble forecast starting from 0600 and 1800 UTC,

¹ Note that the spatial distribution of the other nongrowing (random) part of the first-guess error field is largely unrelated to the atmospheric dynamics and will be ignored in this study.

² The spread in (2) is defined with respect to the control forecast and not the ensemble mean for computational convenience.

we only calculate σ^2 at every 0000 UTC by using all five pairs of 24-h forecast ensemble members. The ratio at 0600, 1200, and 1800 UTC is then computed by linear time interpolation between the two adjacent ratios at 0000 UTC that bracket the analysis time. The small and large scales used in (2) were chosen as in experiment 1 (see below), with values that were assumed to be representative scales of local spread and smooth variation of the analysis errors.

a. Characteristics of the uncertainty ratio and impact on the analysis field and first guess

As indicated in section 2, we set an upper bound of 1 on $1/\sigma^2$ before multiplying the observational errors (i.e., in regions of small forecast errors, the observational errors remain at their nominal value). The distribution of σ^2 varies not only in time but also with the component of the field (temperature, wind, moisture) and vertical level. Figure 1 shows an example of distribution of $1/\sigma^2$ at different sigma levels for the wind field at 0000 UTC 18 June 1996. It shows that there are distinct values of the forecast spread at different vertical levels. The impact of changes in moisture is larger in the Tropics (not shown).

We then introduced the effect of large uncertainties into the NCEP SSI analysis system. The results are compared with a control run that keeps the error covariances constant in time. To verify the quality of the analysis, the RMS fit of both temperature (in K) and vector wind (in $m\ s^{-1}$) against rawinsonde and dropsonde data are presented in Fig. 2 for the analysis field itself and in Fig. 3 for the next first guess, which is the 6-h forecast started from the analysis field. This particular case is verified at the analysis time of 0000 UTC 18 June 1996. The figure shows that the method drives the analysis fields closer to the observations when compared to the control analysis field (as could be expected from the reduction of the observational errors in areas of large forecast uncertainty). However, this improved fit is preserved in the next first-guess field, indicating that the analysis has been improved by this procedure. We have obtained similar results in most cases.

b. Impact of variable uncertainty on medium-range weather forecasts

We first tested the method using the data period 0000 UTC 1 August 1995 to 0000 UTC 14 August 1995. According to the scale of smoothing operators, two experiments were performed: In experiment 1 the large-scale smoothing is taken as $L_H = 1500$ km for horizontal smoothing and $L_V = 4$ km for the vertical. For small-scale smoothing, the horizontal scale is $S_H = 300$ km and the vertical scale $S_V = 1$ km. In experiment 2, we used the same scales except for the large-scale horizontal smoothing, which is taken as $L_H = 2000$ km. We use the obtained ratio to adjust the observation error

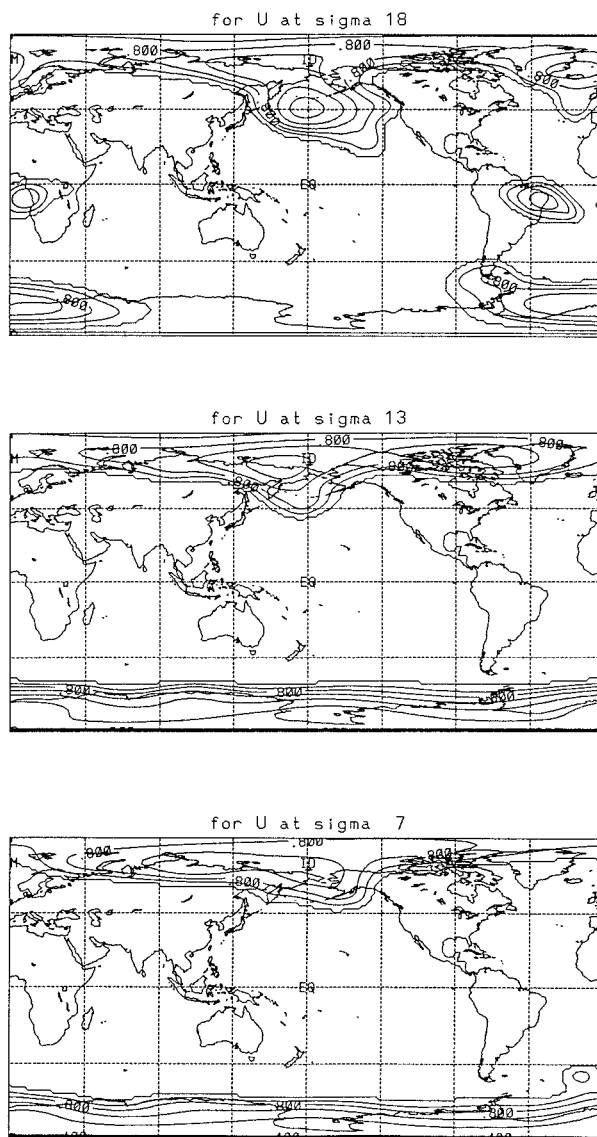


FIG. 1. An example of distribution of $1/\sigma^2$ at different sigma levels. This contour illustrated $1/\sigma^2$ at sigma level 7 (sigma = 0.846), level 13 (sigma = 0.501), and level 18 (sigma = 0.210) for wind field at 0000 UTC 18 June 1996. The contour interval is 0.1.

covariance in the SSI system, then 5-day forecasts from every 0000 UTC analysis field were compared with the corresponding control (operational at T62 resolution) forecast. Table 1 shows the comparison of the 1–5-day forecast average anomaly correlation scores for 500-mb geopotential height. It shows a positive impact of the experiments with respect to the control (which did not account for the time-varying forecast uncertainty), especially the skill of medium-range weather forecasts has been increased. Experiment 2 is slightly better than experiment 1 in the Southern Hemisphere, and it was used for the rest of the experiments presented in the next section.

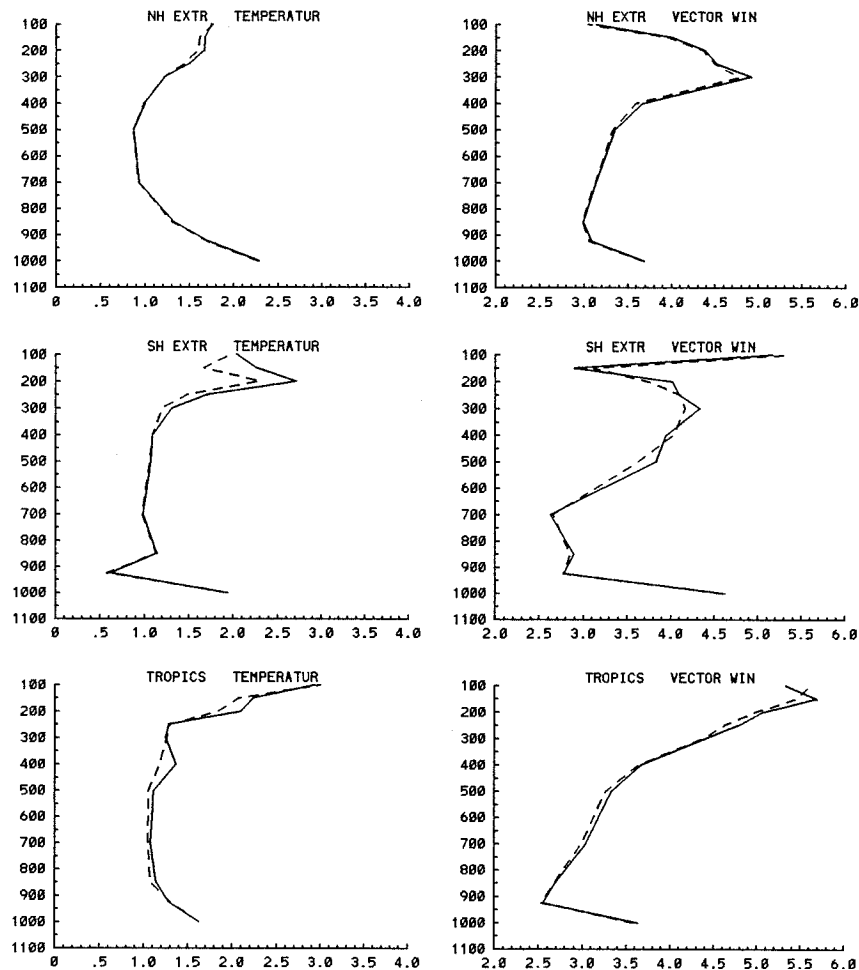


FIG. 2. Root-mean-square fit of temperature and vector wind against the rawinsonde and dropsonde data for the analysis field at 0000 UTC 18 June 1996. The vertical axis denotes the pressure level (unit: hPa), and the horizontal axis denotes the rms error of temperature (unit: K) or vector wind (unit: m s^{-1}). Dashed line for experiment and solid line for control analysis.

4. The results of parallel tests

The method has been tested in parallel within the current NCEP global medium-range weather forecast system starting from 0000 UTC 23 April 1996, comparing as a control with the lower-resolution version (T62/28L) of the NCEP global operational forecast model. The parallel test is designed following experiment 2 in section 3b. As of 0000 UTC 25 June, there were 45 cases available for comparison. Figure 4 shows the 5-day forecast anomaly correlation score for 1000- and 500-mb geopotential height verified against the control analysis. The results indicate that the method improves the medium-range weather forecast for most cases and that the improvement is larger in the SH. Table 2 shows the comparison of the 1–5-day forecast average anomaly correlation scores for geopotential height, demonstrating that the method improves the forecast anomaly correction in both hemispheres at all ranges, except in days 1 and 2 in the Northern Hemisphere.

5. Summary and discussion

This study shows that the use of the bred vectors of the ensemble forecast in the NCEP SSI analysis system has improved the quality of weather forecasts. The method drives the analysis field closer to the observational data in the areas where the ensemble identifies large forecast uncertainty. It also improves the quality of analysis and next guess, as well as the medium-range weather forecast. The method only requires calculating the ratio of the ensemble spread in small and large (continental) scales, and the inverse of this ratio (bounded by 1) is used to adjust the observational errors. The computational cost of this method is negligible, since the ensemble forecasts are already available. The positive impact of the experiments encourages further exploration of the use of the bred vectors in improving the analysis system by taking into account the forecast “errors of the day” rather than assuming that the fore-

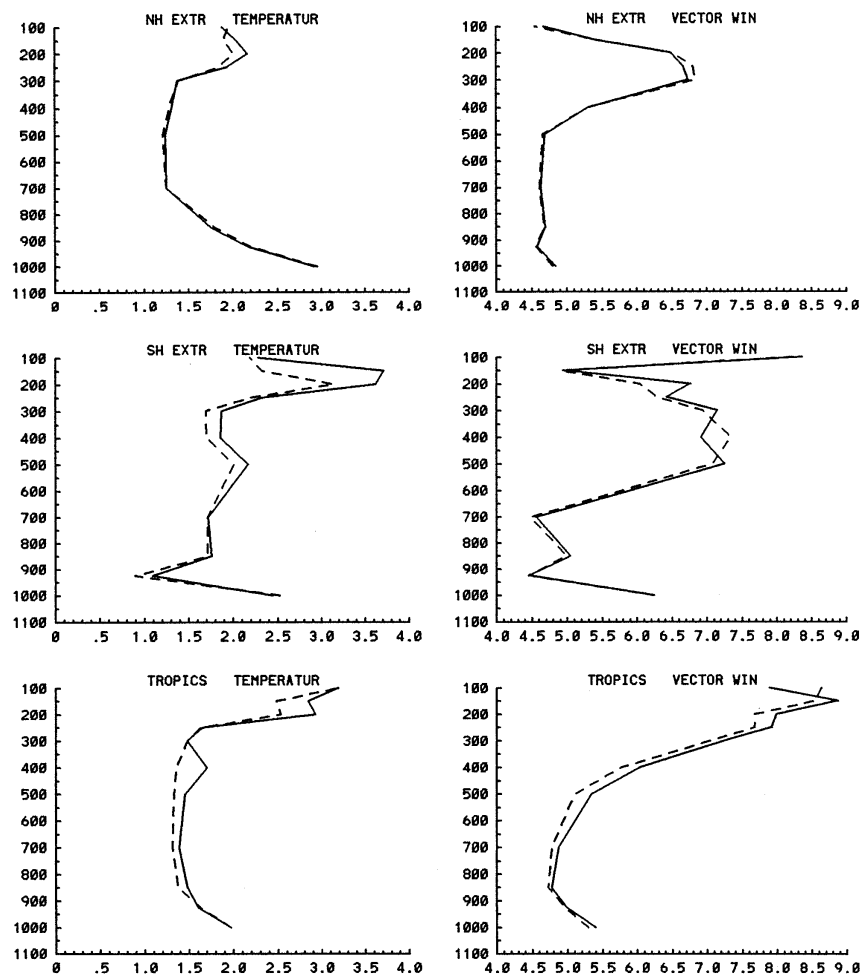


FIG. 3. Same as Fig. 2 except the rms fit for the 6-h forecast.

cast error covariance is constant in time, as currently done in all operational systems.

In this study we used the bred vector in NCEP three-dimensional variational data assimilation by reducing the observational errors in areas identified by the ensemble as areas of large forecast uncertainty. The results suggest that the NCEP bred vectors provide a good representation of growing forecast errors even at the shortest ranges. Other (more advanced) methods to take advantage of this knowledge of the day-to-day variability

in the forecast errors are also possible and will be explored in the future. Two such methods are an improvement of the first guess by minimizing the distance between the first guess and the observations, but moving only along the direction of the bred growing vectors (Kalnay and Toth 1994; Purser et al. 1994), and the inclusion of a flow-dependent forecast error covariance, also based on the ensemble, into the SSI analysis scheme, (J. Derber 1996, personal communication). In the development of the latter method we will build upon the results and the experiences reported in the present paper.

TABLE 1. Comparison of 1–5-day forecast anomaly correlation average score verified against control analysis for 500-mb geopotential heights ($n = 14$ cases, 1–20 waves).

Day	Northern Hemisphere			Southern Hemisphere		
	Ctrl.	Exp+1	Exp+2	Ctrl.	Exp+1	Exp+2
1	0.978	0.978	0.978	0.977	0.977	0.978
2	0.937	0.938	0.938	0.929	0.929	0.930
3	0.872	0.873	0.873	0.862	0.863	0.865
4	0.800	0.803	0.803	0.787	0.790	0.794
5	0.709	0.713	0.710	0.712	0.715	0.722

Acknowledgments. We are most grateful to Drs. Mark Iredell, Peter Caplan, and Hua-Lu Pan for their help in creating the executable for the parallel tests. We also would like to thank Thomas Hamill and two anonymous reviewers for their comments on manuscript. The first author is supported by the UCAR–NCEP Visiting Scientist Program.

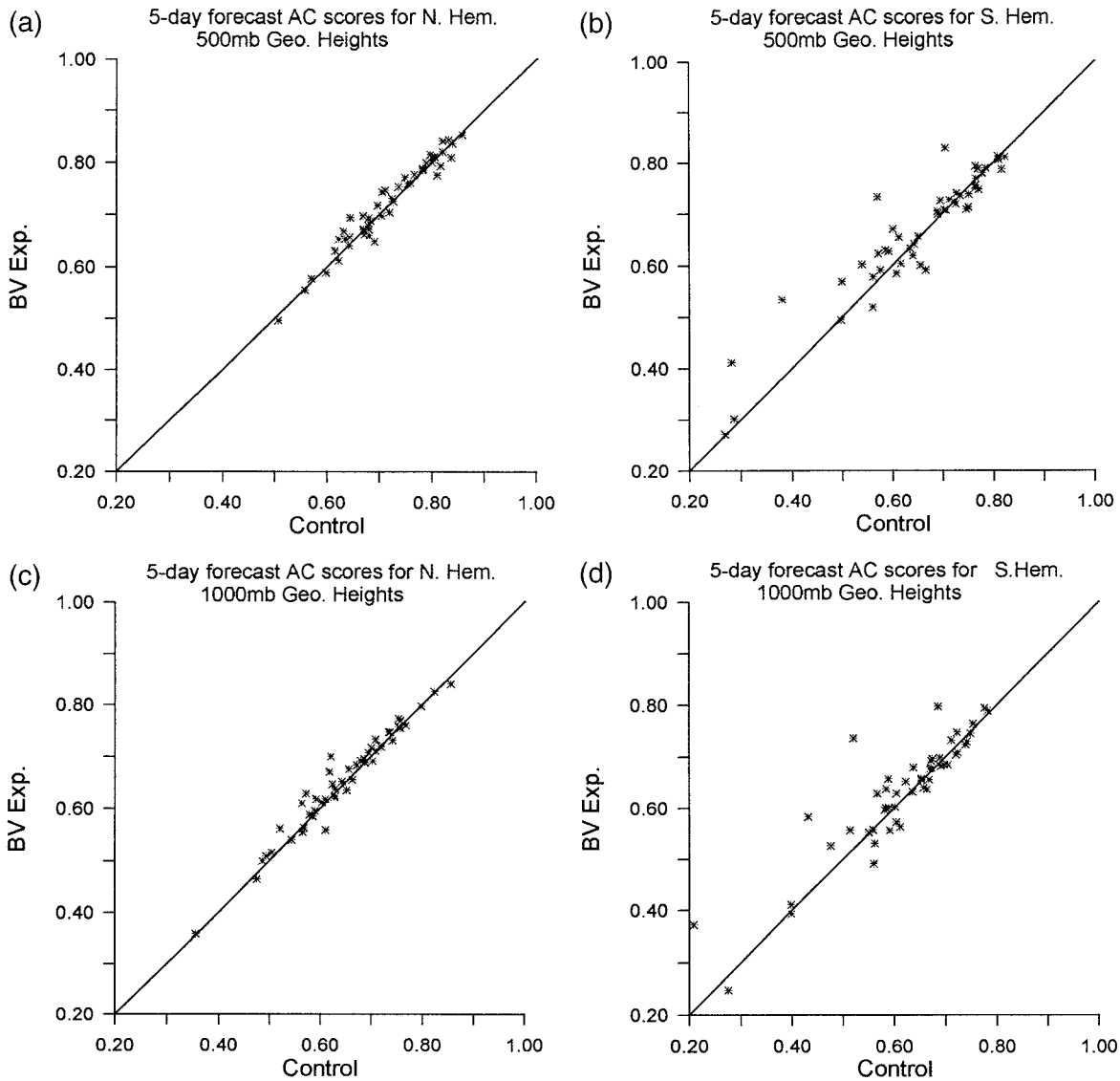


FIG. 4. Scatter diagrams of the 5-day forecast anomaly correlation (AC) scores for geopotential height field in experiment and control forecast: (a) Northern Hemisphere, 500 mb; (b) Southern Hemisphere, 500 mb; (c) Northern Hemisphere, 1000 mb; and (d) Southern Hemisphere, 1000 mb.

TABLE 2. Comparison of 1–5-day forecast anomaly correlation average score verified against the control analysis for 500- and 1000-mb geopotential heights (n = 45 cases, 1–20 waves).

Day	Northern Hemisphere				Southern Hemisphere			
	1000 mb		500 mb		1000 mb		500 mb	
	Ctrl.	Test	Ctrl.	Test	Ctrl.	Test	Ctrl.	Test
1	0.964	0.962	0.983	0.983	0.961	0.961	0.976	0.977
2	0.911	0.910	0.950	0.950	0.899	0.900	0.928	0.931
3	0.853	0.854	0.898	0.899	0.809	0.816	0.850	0.861
4	0.764	0.769	0.822	0.824	0.709	0.727	0.751	0.765
5	0.636	0.644	0.711	0.717	0.604	0.624	0.639	0.652

REFERENCES

Derber, J., and W.-S. Wu, 1996: The use of cloud-cleared radiances in the NCEP's SSI analysis system. Preprints, *11th Conf. on Numerical Weather Prediction*, Norfolk, VA, Amer. Meteor. Soc., 236–237.

—, D. Parrish, and S. J. Lord, 1991: The new global operational analysis system at the National Meteorological Center. *Wea. Forecasting*, **6**, 538–547.

—, —, W.-S. Wu, Z.-X. Pu, and S. Rizvi, 1994: Improvements to the operational SSI global analysis system. Preprints, *10th Conf. on Numerical Weather Prediction*, Portland, OR, Amer. Meteor. Soc., 149–150.

Iyengar, G., Z. Toth, E. Kalnay, and J. Woollen, 1996: Are the bred vectors representative of analysis error? Preprints, *11th Conf. on Numerical Weather Prediction*, Norfolk, VA, Amer. Meteor. Soc., J64–J66.

Kalnay, E., and Z. Toth, 1994: Removing growing errors in the anal-

- ysis. Preprints, *10th Conf. Numerical Weather Prediction*, Portland OR, Amer. Meteor. Soc., 212–215.
- Lorenc, A. C., 1986: Analysis methods for numerical weather prediction. *Quart. J. Roy. Meteor. Soc.*, **112**, 1177–1194.
- Pan, H.-L., J. Derber, D. Parrish, W. Gemmill, S.-Y. Hong, and P. Caplan, 1995: Changes to the 1995 NCEP operational MRF model analysis/forecast system. National Weather Service Tech. Procedures Bull. 428, 30 pp. [Available from NCEP/NWS/NOAA, 5200 Auth Rd., Camp Springs, MD 20746.]
- Parrish, D. F., and J. Derber, 1992: The National Meteorological Center's spectral statistical interpolation analysis system. *Mon. Wea. Rev.*, **120**, 1747–1763.
- , —, J. Purser, W. Wu, and Z. Pu, 1997: The NCEP Global Analysis system: Recent improvements and future plans. *J. Meteor. Soc. Japan*, **75**, 359–365.
- Pu, Z.-X., E. Kalnay, J. Derber, and J. Sela, 1997: Using forecast sensitivity patterns to improve the future forecast skill. *Quart. J. Roy. Meteor. Soc.*, **123**, 1035–1054.
- Purser, R. J., D. F. Parrish, Z. Toth, and E. Kalnay, 1994: Numerical filtering applied to the enhancement of pre-analysis corrections of background errors expressible as rapidly amplifying modes. Preprints, *10th Conf. on Numerical Weather Prediction*, Portland, OR, Amer. Meteor. Soc., 243–244.
- Toth, Z., and E. Kalnay, 1993: Ensemble forecasting at NMC: The generation of initial perturbation. *Bull. Amer. Meteor. Soc.*, **74**, 2317–2330.
- , and —, 1995: Ensemble forecasting at NCEP and the breeding method. NCEP Office Note 407, 55 pp. [Available from NCEP, 5200 Auth Rd., Camp Springs, MD 20746.]
- Wahba, G., D. R. Johnson, F. Gao, and J. Gong, 1995: Adaptive tuning of numerical weather prediction model: Randomized GCV in three- and four-dimensional data assimilation. *Mon. Wea. Rev.*, **123**, 3358–3369.
- Zhu, Y., G. Iyengar, Z. Toth, S. Tracton, and T. Marchok, 1996: Objective evaluation of the NCEP global ensemble forecasting system. Preprints, *11th Conf. on Numerical Weather Prediction*, Norfolk, VA, Amer. Meteor. Soc., J79–J82.

